Both the Structure and DNA Binding Function of the Barrier-to-Autointegration Factor Contribute to Reconstitution of HIV Type 1 Integration in Vitro

THE JOURNAL OF BIOLOGICAL CHEMISTRY
Vol. 275, No. 50, Issue of December 15, pp. 39671–39677, 2000

Printed in U.S.A.

Both the Structure and DNA Binding Function of the Barrier-to-Autointegration Factor Contribute to Reconstitution of HIV Type 1 Integration *in Vitro**

Received for publication, March 28, 2000, and in revised form, September 22, 2000
Published, JBC Papers in Press, September 25, 2000, DOI 10.1074/jbc.M002626200

Dylan Harris and Alan Engelman‡

From the Department of Cancer Immunology and AIDS, Dana-Farber Cancer Institute and the Department of Pathology, Harvard Medical School, Boston, Massachusetts 02115

Retroviral integration is mediated by viral preintegration complexes (PICs), and human immunodeficiency virus type 1 (HIV-1) PICs treated with high salt lose their *in vitro* integration activity. Barrier-to-autointegration factor (BAF) is a host protein that efficiently restores PIC activity, but the mechanism(s) by which BAF participates in HIV-1 integration remains largely unknown. Here we developed a gel shift assay to study BAF DNA binding, and analyzed 14 mutant proteins containing substitutions of conserved residues for binding and PIC reconstitution activities. Although wild-type BAF efficiently bound double-stranded DNA, binding to single-stranded DNA, RNA, or an RNA/DNA hybrid was not detected, suggesting that BAF associates with retroviral cDNA relatively late during reverse transcription. Although some of the BAF mutant proteins efficiently bound DNA, others were defective for binding. Mutants that bound DNA efficiently reconstituted HIV-1 integration, even though in one case binding was just 0.2% of wild-type BAF. Although misfolded mutants did not reconstitute integration, a structurally intact DNA binding-defective mutant displayed partial activity at high BAF concentration. We therefore conclude that both BAF protein structure and its DNA binding activity play roles in reconstituting HIV-1 integration *in vitro*.

Integration of a cDNA copy of the retroviral RNA genome into a host cell chromosome is essential for efficient gene expression and viral replication. The key viral players in integration are the integrase protein, which enters cells as a virion component, and the DNA attachment site, which is comprised of sequences at the ends of the linear cDNA made by reverse transcription. *In vivo*, integration is mediated by large nucleoprotein complexes, termed preintegration complexes (PICs),[1] that are derived from the cores of infecting virions. PICs isolated from infected cells can integrate their endogenous cDNA into an added target DNA *in vitro* (for a review, see Ref. 1).

In addition to the viral integrase, recent studies implicate host-encoded proteins as important cofactors in retroviral cDNA integration. Moloney murine leukemia virus (MMLV) and human immunodeficiency virus type 1 (HIV-1) PICs treated with elevated concentrations of salt and subsequently purified by size exclusion chromatography and nonionic density gradient centrifugation lost their normal intermolecular integration activity (2, 3). Adding back protein extracts of uninfected host cells to such salt-depleted PICs restored normal integration activity, showing that host proteins play essential roles in retroviral PIC function *in vitro* (2–5). Two different proteins, HMG I(Y) (4, 5) and the barrier-to-autointegration factor (BAF) (6), were identified by purifying host cell extracts and assaying for reconstitution of salt-disrupted PIC integration activity *in vitro*. Both HMG I(Y) and BAF display reconstitution activity following their expression and purification from *Escherichia coli* (3–7). For both MMLV and HIV-1, recombinant BAF was about 500-fold more active than recombinant HMG I(Y) at reconstituting the integration activity of salt-washed PICs (3, 5, 7). BAF was not detected in MMLV virions (2, 6), leading to models wherein it associates with retroviruses during the processes of reverse transcription and PIC formation in infected cells (3, 6).

BAF interacts with various components of the inner nuclear membrane, including lamina-associated polypeptide 2 (9) and emerin (10), suggesting that one of its normal physiological roles is aiding reorganization of postmitotic nuclei (9, 10). BAF is an 89-residue nonspecific DNA binding protein that exists as a dimer in solution (6, 8). Although DNA binding is proposed to be important for BAF function in retroviral cDNA integration (6), this has not been experimentally investigated. Here, we established a gel mobility shift assay to study the DNA binding activity of recombinant human BAF. We then engineered recombinant mutant proteins containing substitutions of conserved amino acid residues. Purified mutant proteins were assayed for DNA binding activity by gel mobility shift and reconstitution of integration activity to salt-washed HIV-1 PICs. Each mutant that bound DNA by gel shift efficiently reconstituted HIV-1 integration activity. Because only structurally intact DNA binding-defective mutants displayed PIC reconstitution activity at high BAF concentration, we conclude that the native structure of the BAF protein in addition to its DNA binding function plays a role in reconstituting HIV-1 integration activity *in vitro*.

MATERIALS AND METHODS

Polyacrylamide Gel Mobility Shift Assay—A double-stranded 30-base pair (bp) oligonucleotide substrate was prepared for gel mobility shift as follows. The 5′-end of 5′-GAATCCTAACTGGGCGGAGTTATGCTG-GTG-3′ was labeled with ^{32}P using T4 polynucleotide kinase (Amersham Pharmacia Biotech) as described previously (11). Following heat

* This work was supported by National Institutes of Health Grant AI39394, by funds from the G. Harold and Lelia Y. Mathers Foundation, and by a gift from the Friends 10. The costs of publication of this article were defrayed in part by the payment of page charges. This article must therefore be hereby marked "*advertisement*" in accordance with 18 U.S.C. Section 1734 solely to indicate this fact.

‡ To whom correspondence should be addressed: Dept. of Cancer Immunology and AIDS, Dana-Farber Cancer Institute, 44 Binney St., Boston, MA 02115. Tel.: 617-632-4361; Fax: 617-632-3113; E-mail: alan_engelman@dfci.harvard.edu.

[1] The abbreviations used are: PIC, preintegration complex; MMLV, Moloney murine leukemia virus; HIV-1, human immunodeficiency virus type 1; BAF, barrier-to-autointegration factor; bp, base pair(s); His-tag, hexahistidine tag; kb, kilobase(s); CD, circular dichroism; WT, wild-type; DTT, dithiothreitol.

inactivation of the kinase, the complementary single strand was annealed as described (11). Unincorporated nucleotide was removed by passage over a P6 spin column (Bio-Rad) as described previously (12). For binding assays employing either single-stranded RNA or an RNA/DNA heteroduplex, a synthetic 30 base RNA (5′-CAGGGACAAGC-CCGCGGUGACGAUCUCUAA-3′) was end-labeled, divided into two fractions, and either purified by spin column or first annealed to its cDNA strand prior to spin column chromatography.

DNA binding reactions (50 μl) contained 2% glycerol, 0.01% Triton X-100, 0.5× TBE (44.5 mM Tris base, 44.5 mM borate, 1 mM EDTA, pH 8.3), 0.001% bromphenol blue, and 5 nM nucleic acid substrate. BAF was added last, and DNA binding proceeded for 15 min on ice. Binding reactions were separated on native 5% polyacrylamide gels containing 0.5× TBE. Gels were pre-electrophoresed in 0.5× TBE for 1 h prior to loading, and electrophoresis continued for approximately 2 h until the bromphenol blue dye approached the bottom of the gel. Dried gels were exposed for autoradiography, and protein·DNA complex formation was quantified using either densitometry (IS-1000 Digital Imaging System) or phosphorimaging (PhosphorImager, Molecular Dynamics). DNA binding activity was calculated as the percentage of wild-type protein·DNA complex formation at 50 nM protein. Activities of defective mutants were similarly calculated, with the addition that the percentage of wild-type complex formation was divided by the -fold increase in protein concentration over 50 nM.

Site-directed Mutagenesis—Mutagenesis was performed using the Stratagene QuikChange mutagenesis kit as specified by the manufacturer. The template for mutagenesis was pET15bhBAF (8), a generous gift of Dr. Robert Craigie. This plasmid encodes a 20-residue peptide with a hexahistidine tag (His-Tag) fused to the amino terminus of BAF. The His-tag, which facilitates purification by metal-chelating affinity chromatography (6, 8, 11, 13), was removed from BAF prior to the majority of the *in vitro* DNA binding and integration assays (see below). The presence of mutations, as well as the absence of off-site changes, were confirmed in mutant plasmids by dideoxy sequencing.

Protein Expression and Purification—Wild-type and mutant BAF proteins were expressed in *Escherichia coli* and purified essentially as described previously (8). In brief, protein expression vectors were transformed into BL21(DE3) pLysS (Novagen), and cells were grown in 500 ml of Terrific broth containing 100 μg/ml ampicillin at 37 °C until the optical density at 600 nm was approximately 0.8. Protein expression was induced by adding isopropyl-1-thio-β-D-galactopyranoside to the final concentration of 0.4 mM, and cells were harvested 2.5 h post-induction. The cells were resuspended in 30 ml of ice-cold 25 mM HEPES, pH 7.6, 0.1 mM EDTA, frozen in liquid N_2, and thawed on ice overnight. The remaining steps were performed on ice or at 4 °C. Thawed cells were resuspended in 30 ml of lysis buffer (20 mM HEPES, pH 7.6, 150 mM KCl, 2 mM EDTA, 0.01% lysozyme, 0.1% Triton X-100), incubated for 1 h, and sonicated as described previously (11). The supernatant was discarded after centrifugation at 40,000 × *g*, and the insoluble pellet containing BAF was extracted under denaturing conditions using buffer A (6 M guanidine-HCl, 150 mM KCl, 20 mM HEPES, pH 7.6, 2 mM β-mercaptoethanol, 0.1 mM EDTA, 5 mM imidazole).

BAF was purified using fast protein liquid chromatography (Amersham Pharmacia Biotech). A 2-ml column of chelating Sepharose Fast Flow (Amersham Pharmacia Biotech) was precharged with nickel and equilibrated with buffer A essentially as described previously (11). The cell extract was loaded, and the column was washed with approximately 50 ml of buffer A and then with a similar volume of buffer A containing 20 mM imidazole. The column was developed using a linear gradient of 20 to 600 mM imidazole in buffer A. BAF-containing fractions identified by denaturing polyacrylamide gel electrophoresis were pooled, and EDTA was added to the final concentration of 10 mM. Pooled fractions were dialyzed against buffer B (50 mM potassium phosphate, pH 6.5, 200 mM NaCl, 10 mM EDTA, 5 mM β-mercaptoethanol), the dialysate was cleared by centrifugation at 19,000 × *g* for 10 min, and the concentration of BAF in the supernatant was determined by spectrophotometry using a calculated extinction coefficient (14) of 1.05 ml·mg^{-1} cm^{-1}.

The His-tag was removed by cleavage with thrombin. Thrombin was added to the final concentration of 20 National Institutes of Health units per mg of BAF, and cleavage proceeded for 40 min at room temperature. Thrombin was removed from solution by adsorption to a benzamidine-Sepharose 6B column (Amersham Pharmacia Biotech) as described previously (11). The column eluate was dialyzed against buffer C (20 mM Tris-HCl, pH 7.0, 10% glycerol, 150 mM NaCl, 5 mM DTT, 0.1 mM EDTA), and the concentration of thrombin-cleaved BAF in the clarified dialysate was calculated using an extinction coefficient of 1.24 ml·mg^{-1} cm^{-1}. BAF was frozen in liquid N_2 and stored at −80 °C.

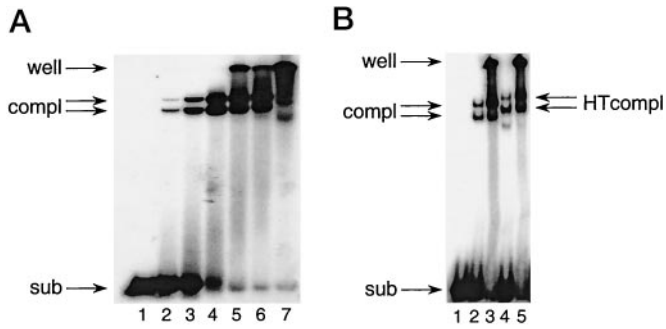

FIG. 1. **BAF DNA binding activity by polyacrylamide gel mobility shift.** *A*, BAF was omitted from the DNA binding reaction in *lane 1*; *lane 2* contained 10 nM BAF; *lane 3*, 20 nM; *lane 4*, 50 nM; *lane 5*, 100 nM; *lane 6*, 250 nM; *lane 7*, 1.25 μM. The *arrows* to the left of the gel indicate the gel well, and the migration positions of the BAF·DNA complexes (*compl*) and free DNA substrate (*sub*). *B*, BAF was omitted from the binding reaction in *lane 1*; the reaction in *lane 2* contained 10 nM BAF; *lane 3*, 50 nM BAF; *lane 4*, 10 nM His-tag BAF; *lane 5*, 50 nM His-tag BAF. The migration position of the His-tag protein·DNA complexes are marked *HTcompl*; other labeling is the same as in *A*.

Thrombin cleavage yields the sequence Gly-Ser-His-Met at the amino terminus, where Met is the predicted terminus of endogenous human BAF (8).

HIV-1 Infection, Isolation of PICs, Salt Stripping, and Integration Assays—SupT1 and MOLTIIIB cells were grown in RPMI medium supplemented with 10% fetal calf serum. SupT1 cells were infected by coculture with chronically infected MOLTIIIB cells as described previously (3, 15). PICs were isolated, incubated with 1.2 M KCl for salt stripping, purified by spin column chromatography, and then by Nycodenz gradient centrifugation as described (3, 15). Integration and PIC reconstitution assays using 100 or 500 ng of purified BAF protein were performed, separated on agarose gels, and analyzed by Southern blotting also as described previously (3, 15). Southern blots were processed for autoradiography, and integration activity was quantified by densitometry or by phosphorimaging. Integration activity was calculated as the percentage of the 9.7-kilobase (kb) HIV-1 cDNA substrate that was converted into the 15.1-kb integration product. Mutant BAF reconstitution activity was calculated as the percentage of wild-type BAF activity. Mutants were analyzed in at least two independent experiments.

Gel Filtration Chromatography—The multimeric state of recombinant BAF was analyzed by fast protein liquid chromatography using a Superdex 200 HR 10/30 column (Amersham Pharmacia Biotech). The column was calibrated by analyzing the elution profiles of molecular mass standards (Bio-Rad) in buffer D (20 mM Tris-HCl, pH 7.5, 1 mM EDTA, 50 mM KCl, 6% sucrose, 1 mM DTT). The retention times of BAF (0.3–0.4 mg) were analyzed under the same conditions. The dimeric and higher order multimeric species of wild-type BAF were collected separately and concentrated by ultrafiltration using a Centricon 3 concentrator (Amicon). Concentrated samples were dialyzed against buffer C prior to gel mobility shift assays and gel filtration chromatography.

Circular Dichroism (CD)—The CD spectra of BAF proteins (0.3 mg/ml) in buffer E (50 mM potassium phosphate, pH 7.5, 50 mM KCl, 0.1 mM EDTA, 1 mM DTT, 5% glycerol) were recorded on an AVIV 62DS spectropolarimeter. Measurements in the far-UV region (260–190 nm) were made using a 0.1-cm path length cell.

RESULTS AND DISCUSSION

DNA Binding Activity by Gel Mobility Shift—BAF is a nonspecific host cell DNA binding protein (6) that efficiently restores intermolecular integration activity to salt-stripped MMLV (6) and HIV-1 (3) PICs *in vitro*. A polyacrylamide gel mobility shift assay was established to investigate the nucleic acid binding properties of recombinant human BAF purified following its expression in *E. coli*. A 30-bp oligonucleotide of random sequence was chosen as the substrate for DNA binding. Preliminary experiments revealed that the presence of low concentrations of glycerol and nonionic detergent in the binding buffer, and electrophoresis at room temperature as opposed to 4 °C, yielded two protein·DNA complexes with distinct electrophoretic mobilities (Fig. 1*A* and data not shown). Although a protein concentration of 10 nM BAF monomer was sufficient for

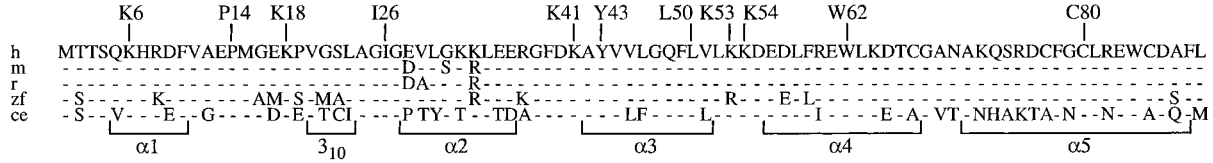

FIG. 2. **Amino acid sequence alignment and identification of targeted residues.** The primary amino acid sequences of human (*h*), mouse (*m*), rat (*r*), zebrafish (*zb*), and *C. elegans* (*ce*) BAF are shown. The human, mouse, zebrafish, and *C. elegans* sequences were from Ref. 8, and the rat sequence was from Ref. 9. *Dashes* indicate the positions of amino acid identity. Residues chosen for mutagenesis are noted above the human sequence, and the locations of the five α-helices and 3_{10}-helical turn in the BAF solution structure (8) are noted below the *C. elegans* sequence. That study revealed that most of the residues important for dimerization reside in helix 3, and helices 4 and 5 comprise a helix-turn-helix motif important for DNA binding.

complex formation (Fig. 1*A*, *lane 2*), 50–100 nM BAF retarded the mobility of virtually all of the DNA substrate, yielding some aggregated material in the well of the gel (Fig. 1*A*, *lane 5*, and 1*B*, *lane 3*). We previously determined that BAF concentrations in the range of 5 to 50 nM efficiently reconstituted the integration activity of salt-depleted HIV-1 PICs *in vitro* (3). Thus, we conclude that the protein·DNA complexes observed by gel mobility shift are relevant to BAF's cofactor role in HIV-1 integration. Increasing the concentration of BAF in the DNA binding reaction yielded a series of novel species, most of which displayed slower electrophoretic mobilities than the two complexes that were observed at lower concentrations (Fig. 1*A*, compare *lanes 6* and *7* to *lanes 2–4*). Because we previously determined that BAF concentrations greater than approximately 250 nM inhibited functional reconstitution of salt-stripped PICs (Ref. 3 and data not shown), we speculate that the protein·DNA aggregates and novel complexes observed by gel mobility shift at high BAF concentrations are not relevant to HIV-1 integration.

To investigate whether the observed protein·DNA complexes were due to the DNA binding activity of human BAF and not potentially contaminating *E. coli* proteins, DNA binding reactions were repeated using purified BAF protein still containing the His-tag. Because the His-tag was removed as a 17-residue thrombin cleavage product, we reasoned that the larger size of the His-tag protein might yield protein·DNA complexes displaying slower electrophoretic mobilities than those formed with the proteolyzed protein. Although the presence of the His-tag yielded a minor novel species (Fig. 1*B*, *lane 4*), it is clear that it retarded the mobility of the two protein·DNA complexes that formed using thrombin-cleaved BAF (Fig. 1*B*, compare *lanes 4* and *5* to *lanes 2* and *3*). We therefore conclude that the protein·DNA complexes observed by gel mobility shift are due to the DNA binding activity of human BAF protein. The stoichiometries of BAF to DNA in the different nucleoprotein complexes were not investigated.

Only uninfected cell extracts, and not extracts of purified virions, restore intermolecular integration activity to salt-washed MMLV PICs (2). Western blotting also failed to detect BAF in MMLV virions (6), leading to the hypothesis that BAF is recruited to nascent cDNA during reverse transcription and PIC formation in the cytoplasm of infected cells (6). Reverse transcription is a multistep process, and various nucleic acid species, including single-stranded DNA and RNA/DNA hybrids, are generated from single-stranded RNA templates en route to the linear double-stranded cDNA product (16). To investigate whether BAF may have binding affinity for either the RNA template or these DNA synthesis intermediates, single-stranded RNA, single-stranded DNA, and an RNA/DNA hybrid were analyzed in the gel mobility shift assay. BAF did not show detectable levels of binding to any of these nucleic acid substrates (data not shown). The absence of detectable binding to single-stranded RNA is consistent with the absence of BAF in virions (2, 6), and the lack of binding to the RNA/DNA hybrid and single-stranded DNA implies that BAF associates with nascent cDNA relatively late in the reverse transcription process.

Mutagenesis Strategy and Mutant BAF DNA Binding Activity—At the outset of this project, we had knowledge of the primary sequences of mouse, human, and *Caenorhabditis elegans* BAF.[2] Due to the absence of structural data for BAF at this point, amino acid residues were chosen for mutagenesis on the basis of absolute conservation across these three species. Forty-seven amino acids of the 89-residue protein (52.8% identity) are invariant in an expanded alignment that includes rat and zebrafish, and 10 of the 11 residues we chose for mutagenesis are identical across these five species (Fig. 2). Six of the 47 invariant residues, Lys-6, His-7, Lys-18, Lys-41, Lys-54, and Lys-64, are positively charged and therefore could potentially interact nonspecifically with DNA through the phosphodiester backbone. Four of these charged residues, Lys-6, Lys-18, Lys-41, and Lys-54, were included in our mutant set (Fig. 2). Hydrophobic residues Ile-26, Leu-50, and Trp-62 were chosen for their potential roles in BAF·BAF protein interactions, and Pro-14, Tyr-43, and Cys-80 were targeted because these were the only invariant representatives of these residues in the sequence alignment (Fig. 2). The double mutant C80A/R82A, inadvertently generated during mutagenesis, was examined alongside the other single amino acid BAF mutant proteins.

Fourteen different mutant proteins were purified following expression in *E. coli* (Table I). Preliminary DNA binding experiments analyzed mutants at 50 nM protein, because this concentration of wild-type BAF shifted the majority of the double-stranded DNA substrate (Fig. 1*A*, *lane 4*, and 1*B*, *lane 3*). Five of the mutant proteins, P14A, W62A, K41A, K53A, and K54A, supported 20–100% of the wild-type level of DNA binding activity (Fig. 3*A* and Table I). Although the binding of P14A to DNA was indistinguishable from the activity of wild-type BAF (Fig. 3*A*, compare *lane 3* to *lane 2*), W62A bound DNA about one-half as efficiently as did wild-type in repeated experiments (Fig. 3*A*, *lane 7*, and Table I). K41A, K53A, and K54A each bound DNA about one-third as efficiently as did wild-type BAF (Fig. 3*A* and Table I). Thus, two of the invariant lysine residues that we targeted, Lys-41 and Lys-54 (Fig. 2), are not essential for BAF DNA binding activity under these conditions. Similar to the results reported here, K53E was previously reported to display reduced DNA binding activity (8). In contrast, K54E did not support detectable levels of DNA binding (8). It is possible that substituting Glu for Lys-54 had a negative impact on the overall structure of the BAF dimer as compared with the less disruptive Ala residue tested here.

Four of the BAF mutants, Y43A, L50A, C80A, C80A/R82A, displayed 5–20% of the wild-type level of DNA binding activity (Fig. 3*B* and Table I). In repeated experiments, C80A/R82A supported the formation of only the more slowly migrating of

[2] R. Craigie, personal communication.

TABLE I
Summary of BAF mutant proteins

Protein	DNA binding[a]	PIC reconstitution[b]	Multimer[c]
Wild-type	+++	++	D/H
P14A	+++	++	ND
W62A	+++	++	ND
K41A	++	++	ND
K53A	++	++	ND
K54A	++	++	ND
Y43A	+	++	D
L50A	+	++	D/H
C80A	+	++	D/H
C80A/R82A	+	++	D
K18A	+/−	++	D/H
K6A	−	+	D/H
I26A	−	−	H
I26K	−	−	H
L50K	−	−	?

[a] +++, 50–100% of wild-type activity; ++, 20–50% of wild-type activity; +, 2–20% activity; +/−, 0.01–2% activity; −, <0.01% activity. Values are averages of at least two independent measurements.

[b] ++, ≥50% of wild-type activity using 40 nM BAF; +, activity only observed using 200 nM BAF; −, undetectable (<2%) activity.

[c] Predominant multimeric forms detected by gel filtration. D/H, dimers and higher order multimers; D, dimers; H, higher order multimers; ND, not determined; ?, this profile was not consistent with either the wild-type dimers or higher order multimers (Fig. 4).

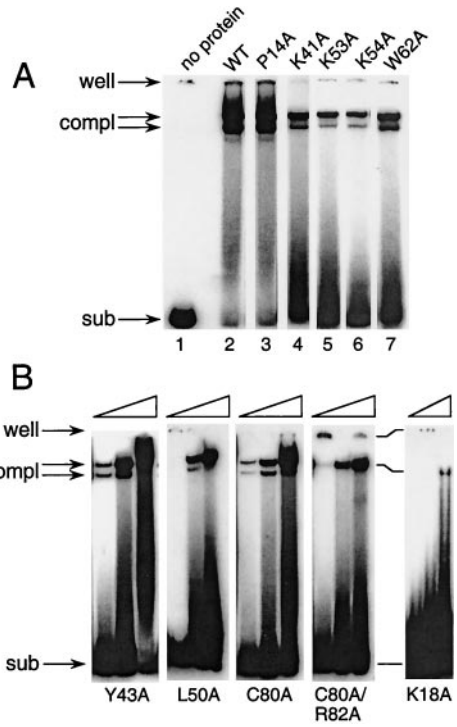

FIG. 3. **DNA binding activity of mutant BAF proteins.** *A*, BAF was omitted from the reaction in *lane 1*. *Lanes 2–7* contained 50 nM wild-type (*WT*), P14A, K41A, K53A, K54A, and W62A BAF, respectively. Other labeling is as in Fig. 1. *B*, Each panel contains three lanes of the indicated mutant tested at the protein concentrations 0.05, 0.25, and 1.25 μM; the *triangles* above the gels depict this increase in protein concentration across the lanes. K18A BAF was analyzed on a separate polyacrylamide gel. Other labeling is as in Fig. 1.

the two protein·DNA complexes observed using wild-type BAF (Fig. 3*B*). K18A also supported formation of just the more slowly migrating nucleoprotein complex, but in this case DNA binding activity was only about 0.2% the level of wild-type BAF (Fig. 3*B* and Table I). This is the first report that invariant residue Lys-18 plays a role in the binding of BAF protein to DNA.

Four of the mutant proteins, K6A, I26K, I26A, and L50K,

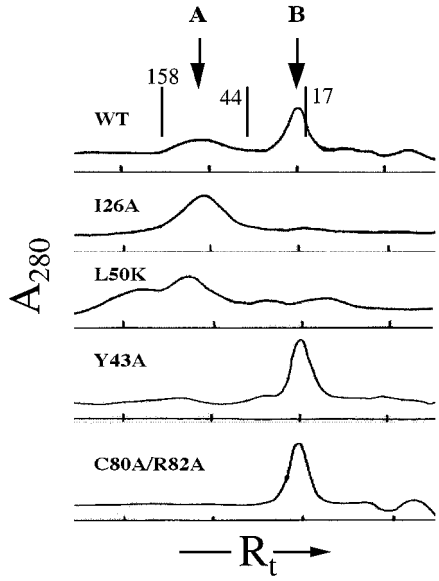

FIG. 4. **Gel filtration chromatography of wild-type and mutant BAF proteins.** The elution profiles of BAF mutants I26A, L50K, Y43A, and C80A/R82A are shown relative to the wild-type chromatogram. Absorbance at 280 nm (A_{280}) was plotted against relative retention time (R_t). Wild-type eluted at two predominant positions, which, based on migration distance relative to molecular mass standards, were consistent with either hexameric or octameric (indicated by *A*) and dimeric (*B*) BAF. *Vertical lines* indicate the retention times of 158-, 44-, and 17-kDa molecular mass standards.

failed to support detectable levels of DNA binding, even when assayed at the elevated protein concentration of 1.25 μM (Table I). One of these mutants, K6A, carries Ala in place of an invariant Lys residue (Fig. 2), and K6E was previously reported defective for DNA binding (8).

Gel Filtration Analysis of BAF Proteins—The results of the previous experiments revealed that, although some of the recombinant BAF mutant proteins bound DNA similarly to wild-type, others were significantly reduced or completely defective for DNA binding activity (Table I). The observed DNA binding defects could be due to either protein structure changes caused by the mutations, removal of side chains critical for binding without perturbing the overall structure of the globular protein, or a combination of both of these reasons. To address this, wild-type BAF and mutants defective for DNA binding were analyzed by gel filtration chromatography and CD spectroscopy (see below). Mutants suffering structural changes would be expected to display gel filtration profiles and/or CD spectra altered from those of the wild-type protein.

Wild-type BAF eluted as two distinct populations from the gel filtration column, the smaller of which displayed a retention time slightly faster than that of a 17-kDa molecular mass standard (Fig. 4). Because thrombin-cleaved BAF has a predicted mass of 10.3 kDa, it appears that this species is dimeric BAF. Consistent with this interpretation, recombinant human BAF analyzed by sedimentation equilibrium and gel filtration was previously reported as dimeric (8). The larger BAF species eluted from the column between 158- and 44-kDa mass standards (Fig. 4). Assuming that this species is a higher order multimer of dimeric BAF, it appeared by this analysis to be either hexameric or octameric. The precise number of BAF protomers in this higher order multimer was not investigated further.

Mutant BAF proteins that displayed greatly reduced DNA binding activity, as well as those completely devoid of DNA binding, were analyzed next. Although two of the mutants that displayed reduced binding, Y43A and C80A/R82A, yielded pri-

marily dimeric protein (Fig. 4 and Table I), two of the DNA binding-defective proteins, I26A and I26K, yielded mostly the higher order multimer (Fig. 4 and Table I). Based on the gel filtration profiles of these four mutant proteins, we next tested whether DNA binding required pre-existing BAF dimers in solution. Column fractions containing dimers and higher order multimers of wild-type BAF were collected separately, concentrated by ultrafiltration, and re-analyzed by gel filtration and gel mobility shift. Wild-type dimers and higher order multimers retained their starting multimeric state during this second round of column chromatography, showing that the different multimeric forms were relatively stable (data not shown). Dimers and higher order multimers displayed similar levels of DNA binding activity, each forming both of the previously noted wild-type protein·DNA complexes in native polyacrylamide gels (data not shown). Thus, each of the multimeric forms probably contributes to the DNA binding activity of the wild-type protein, and the lack of I26A and I26K dimers does not *per se* explain the DNA binding-defective phenotype of these mutant proteins. The results of CD spectroscopy suggest that these mutants were defective due to alterations in protein structure (see below).

The gel filtration profile of L50K differed significantly from the wild-type pattern (Fig. 4), suggesting that this mutation altered the ability of BAF to properly multimerize in solution. In contrast, L50A, C80A, and K18A, each of which supported reduced DNA binding activity, as well as the DNA binding-defective mutant K6A, yielded the wild-type gel filtration pattern of dimers and higher order multimers (Table I). Because L50A contained the wild-type ratio of BAF multimers, we conclude that the L50K multimerization defect is due to the presence of a disruptive Lys residue, as opposed to the absence of the Leu normally at this position. This interpretation is consistent with the location of Leu-50 at the dimer interface in the solution structure of the BAF dimer (8). Unlike the Lys substitution, substituting Ala for Leu-50 apparently did not grossly affect BAF·BAF protein interactions. Tyr-43 and Lys-53 are also located at the dimer interface (8), suggesting that the 3- to 10-fold reductions in DNA binding activity observed with Y43A, L50A, and K53A (Fig. 3 and Table I) could be due to small changes in dimer stability that were undetectable by gel filtration chromatography. The reduced DNA binding activity of K53E was likewise suggested to be due to an alteration in dimer stability (8).

CD Spectra of Wild-type and BAF Mutant Proteins—Three of the DNA binding-defective mutants, I26A, I26K, and L50K, stood out because each of these lacked dimeric BAF as detected by gel filtration chromatography (Fig. 4 and Table I). Thus, CD spectroscopy was used to further analyze the structure of these mutant proteins, as well as the other DNA binding-defective mutant, K6A. Wild-type BAF yielded a CD spectrum typical of α-helical proteins (Fig. 5), displaying minima at or near far-UV wavelengths of 208 and 222 nm (17). I26A and I26K each displayed less minima in these regions, indicating that these proteins contain less overall helical content than does wild-type BAF (Fig. 5 and data not shown). Changes at Ile-26 apparently perturb BAF protein structure, suggesting that I26A and I26K are defective for DNA binding because of these alterations. This interpretation is consistent with the location of Ile-26 in the hydrophobic core of the BAF monomer (8). Presumably, replacing this conserved residue with either Ala or Lys changed the hydrophobicity of the core, which altered the native structure of BAF (Fig. 5). Trp-62 and Cys-80 also form part of the BAF hydrophobic core (8). Replacing either of these invariant residues with Ala did not appear to have the same negative impact on BAF protein structure as did the I26A substitution (Table I).

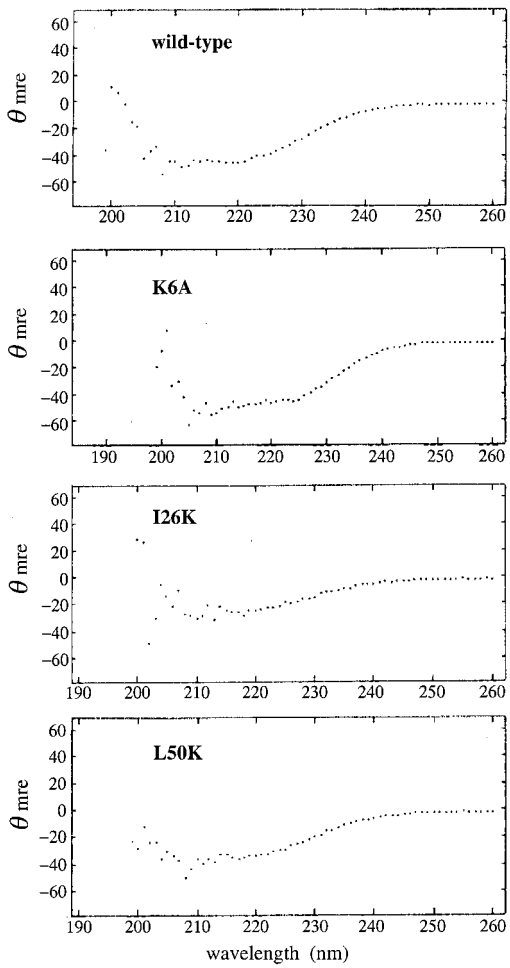

FIG. 5. **CD spectroscopy of wild-type and mutant BAF proteins.** The mean residue ellipticity (θ_{mre}) of the indicated protein is plotted against wavelength. θ_{mre} is in units of 10^{-3} deg·cm^2·dmol^{-1}.

L50K also displayed a CD spectrum with less intense far-UV minima at 208 and 222 nm than did wild-type BAF, although this mutant appeared more similar to wild-type than did either I26A or I26K (Fig. 5 and data not shown). L50K apparently suffers both multimerization (Fig. 4) and protein structure defects (Fig. 5), although it is unclear from these data whether the inability to properly multimerize precluded proper folding, or vice versa.

In contrast to the other DNA binding-defective mutants, the CD spectrum of K6A was very similar to that of wild-type BAF (Fig. 5). K6A appeared wild-type both by gel filtration (Table I) and CD spectroscopy (Fig. 5), yet was completely defective for DNA binding as detected by gel mobility shift (Table I). We therefore suggest that Lys-6 is critical for BAF DNA binding activity, because it directly interacts with DNA. This conclusion is consistent with a model of BAF DNA binding based on previous structural and mutagenic data (8). Here, we additionally measured biophysical properties of purified BAF mutant proteins, experiments whose results were required to conclude that a particular DNA binding mutant was defective solely due to its inability to bind DNA.

Restoration of Integration Activity to Salt-stripped HIV-1 PICs—PICs treated with 1.2 M KCl and subsequently purified by size exclusion and Nycodenz gradient centrifugation lose their ability to integrate HIV-1 cDNA *in vitro*, and recombinant human BAF efficiently restores *in vitro* integration activity to salt-washed HIV-1 PICs (3). The results of gel mobility shift experiments revealed a variety of DNA binding phenotypes,

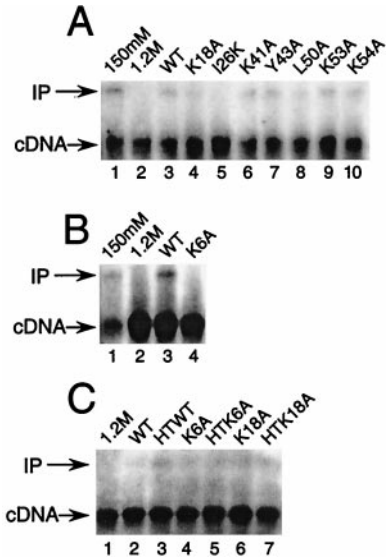

FIG. 6. **Reconstitution of integration activity to salt-washed HIV-1 PICs.** *A*, PICs isolated from infected cells were either treated with 1.2 M KCl (*lane 2*) or mock treated (*lane 1*) prior to spin column chromatography, Nycodenz gradient centrifugation, and *in vitro* integration assays. Although wild-type (*WT*) BAF was added to the PIC reconstitution assay in *lane 3*, the reactions in *lanes 4–10* contained the indicated mutant proteins. *B*, *lane 1* contained gradient-purified mock treated PICs; *lane 2*, PICs were treated with high salt prior to purification; *lane 3*, wild-type BAF in the reconstitution assay; *lane 4*, K6A BAF. The cDNA substrate band is more intense in *lanes 2–4* because 3-fold more material was loaded in these lanes. *C*, *lane 1* contained salt-stripped PICs; *lanes 2–7* contained the indicated thrombin-cleaved or His-tag (*HT*) protein at 200 nM BAF. cDNA, 9.7-kb HIV-1 integration substrate; IP, 15.1-kb integration product.

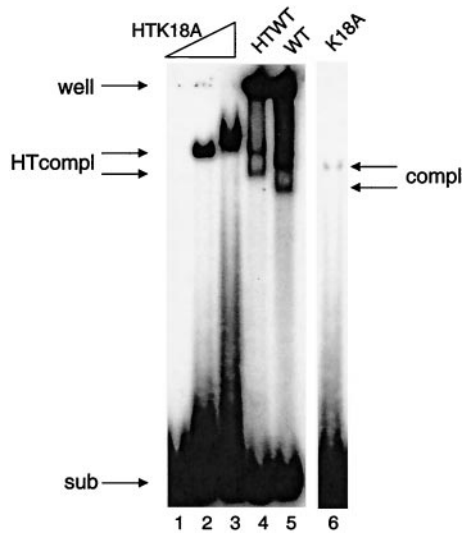

FIG. 7. **The His-tag greatly enhances the DNA binding activity of K18A BAF.** *Lane 1* contained 50 nM His-tag K18A BAF (*HTK18A*); *lane 2*, 250 nM HTK18A; *lane 3*, 1.25 μM HTK18A; *lane 4*, 50 nM His-tag wild-type BAF (*HTWT*); *lane 5*, 50 nM wild-type BAF; *lane 6*, 1.25 μM K18A BAF. Note that although the nucleoprotein complex containing K18A BAF in *lane 6* comigrated with the more slowly migrating wild-type complex in *lane 5*, the His-tag K18A complex in *lanes 2* and *3* comigrated with just the larger of the two complexes formed using the His-tag wild-type protein (*lane 4*). Other labeling is the same as in Fig. 1.

which ranged from undetectable levels of DNA binding to the wild-type level of activity (Fig. 3 and Table I). Each of the purified mutant proteins was next tested alongside wild-type BAF for PIC reconstitution activity.

As expected, treating HIV-1 PICs with 1.2 M KCl prior to purification abolished *in vitro* integration activity (Fig. 6, *A* and *B*, compare *lanes 2* to *lanes 1*). Also as previously reported (3), 100 ng of purified protein, corresponding to approximately 40 nM of wild-type BAF, restored about one-half of the level of integration activity that was present prior to salt-stripping (Fig. 6, *A* and *B*, compare *lanes 3* to *lanes 1*).

Each of the BAF mutants was initially assayed for PIC reconstitution activity at 40 nM protein. Although each of the mutants that bound DNA by gel mobility shift supported efficient PIC reconstitution activity under this condition, none of the DNA binding-defective mutants were active (Fig. 6, *A* and *B*, and Table I). Thus, the DNA binding activity of human BAF protein is important for its ability to efficiently restore integration activity to salt-stripped HIV-1 PICs *in vitro*. Because mutants C80A/R82A and K18A displayed efficient reconstitution activity (Table I), we conclude that the ability to form just the larger of the two nucleoprotein complexes by gel shift is sufficient for BAF function in the PIC reconstitution assay (Fig. 3*B*).

Many of the BAF mutants were quantitatively more active in the PIC reconstitution assay as compared with the gel mobility shift assay (Table I). This was most evident for K18A: This mutant displayed only 0.2% of the wild-type protein's gel shift activity, yet in repeated experiments it reconstituted about the same level of HIV-1 integration activity as did wild-type BAF (Fig. 6*A*, compare *lanes 4* to *lane 3*, Table I). Thus, efficient DNA binding activity as measured by gel mobility shift is not required for efficient reconstitution of salt-stripped HIV-1 PIC integration activity under these assay conditions.

We next analyzed the BAF mutants that were completely defective for DNA binding activity using 500 ng of purified protein, which corresponded to approximately 200 nM BAF, in the PIC reconstitution assay. As previously eluted to, this level of wild-type BAF was somewhat inhibitory for restoring integration activity (Fig. 6*C*, *lane 2*); repeated experiments revealed that 200 nM BAF restored about 50% of the level of PIC activity that was accomplished using 40 nM protein. K18A BAF, which functioned similarly to wild-type at 40 nM protein, also acted similar to the wild-type at 200 nM BAF (Fig. 6*C*, compare *lane 6* to *lane 2*). Surprisingly, K6A restored about the same level of integration activity as wild-type BAF using this assay condition (Fig. 6*C*, compare *lane 4* to *lanes 2* and *6*). Unlike K6A, the other DNA binding-defective mutants, I26A, I26K, and L50K, did not support detectable levels of PIC reconstitution activity under this condition (Table I and data not shown). Because K6A displayed a gel filtration profile and CD spectrum similar to wild-type (Fig. 5 and Table I), and these other defective mutants displayed altered gel filtration profiles (Fig. 4 and Table I) and CD spectra (Fig. 5), our results indicate that the native structure of human BAF protein in addition to its DNA binding function plays a role in restoring integration activity to salt-depleted HIV-1 PICs *in vitro*.

We did not anticipate that mutants K18A and K6A, which displayed gel shift activities of 0.2% and <0.01% of wild-type BAF, respectively, would function in the PIC reconstitution assay. It therefore seems likely that BAF interacts with a component(s) of salt-stripped HIV-1 PICs in addition to the cDNA itself, and this interaction quantitatively increases reconstitution activity as compared with the free DNA binding activity that was measured by gel mobility shift. Although an elevated concentration of K6A was required to detect PIC reconstitution activity (Fig. 6, *B* and *C*), K18A restored HIV-1 integration activity as efficiently as wild-type BAF (Fig. 6*A* and Table I). Thus, the extremely weak DNA binding activity of K18A appears to make it a significantly better cofactor than K6A for functional reconstitution of HIV-1 integration. We noticed that the presence of the amino-terminal His-tag in-

creased the DNA binding activity of K18A approximately 50-fold over that observed using the thrombin-cleaved protein (Fig. 7, compare *lanes 2* and *3* to *lane 6*). This stimulation is not novel to the BAF protein, as the His-tag was previously observed to significantly enhance weak DNA binding activities of certain deletion mutants of recombinant HIV-1 integrase (18) and the catalytic activities of recombinant HIV-1 RNase H (19). We suggest that this artificial stimulation of DNA binding activity correlates with the efficiency of K18A function in the reconstitution assay and speculate that an analogous stimulation in binding activity may occur when K18A BAF interacts with certain components of salt-stripped HIV-1 PICs. Consistent with this interpretation, K6A BAF, which was 5- to 10-fold less active than K18A in the PIC reconstitution assay (Fig. 6 and Table I), remained inactive for DNA binding when assayed as a His-tag protein (data not shown). We note that the His-tag did not stimulate either K6A or K18A reconstitution activity at either 40 nM (data not shown) or 200 nM (Fig. 6*C*) BAF.

How might K6A function in HIV-1 integration in the absence of detectable DNA binding activity? As eluted to, one possibility is that protein components present in salt-stripped PICs enhance the binding of K6A BAF to HIV-1 DNA. Alternatively, K6A might function in the PIC reconstitution assay without directly binding to DNA. In this scenario, endogenous BAF's DNA binding activity was required for PIC formation *in vivo*, but once formed other protein components in addition to BAF contribute to the native integration-competent structure of the PIC. Salt stripping, which inactivates PIC function, presumably removes BAF protein. We speculate that some aspect of native PIC structure remains after salt treatment, and K6A BAF, although unable to bind DNA by itself, partially filled a void left behind by the endogenous BAF protein and in doing so partially reconstituted PIC function. Although speculative, this model is consistent with the observation that viral integrase, which catalyzes the chemical steps of integration, remains PIC-associated following salt stripping (2–7). Experiments are currently underway to further define BAF's role in HIV-1 integration.

Acknowledgments—We thank R. Craigie for pET15b-hBAF plasmid DNA and sharing results prior to publication, V. N. Pandey for the synthetic 30 base RNA oligonucleotide, and H. Chen for a critical review of the manuscript.

REFERENCES

1. Brown, P. O. (1997) *Retroviruses* (Coffin, J. M., Hughes, S. H., Varmus, H. E., eds) pp. 161–203, Cold Spring Harbor Laboratory, Cold Spring Harbor, NY
2. Lee, M. S., and Craigie, R. (1994) *Proc. Natl. Acad. Sci. U. S. A.* **91,** 9823–9827
3. Chen, H., and Engelman, A. (1998) *Proc. Natl. Acad. Sci. U. S. A.* **95,** 15270–15274
4. Farnet, C. M., and Bushman, F. D. (1997) *Cell* **88,** 483–492
5. Li, L., Farnet, C. M., Anderson, W. F., and Bushman, F. D. (1998) *J. Virol.* **72,** 2125–2131
6. Lee, M. S., and Craigie, R. (1998) *Proc. Natl. Acad. Sci. U. S. A.* **95,** 1528–1533
7. Wei, S.-Q., Mizuuchi, K., and Craigie, R. (1998) *Proc. Natl. Acad. Sci. U. S. A.* **95,** 10535–10540
8. Cai, M., Huang, Y., Zheng, R., Wei, S.-Q., Ghirlando, R., Lee, M. S., Craigie, R., Gronenborn, A. M., and Clore, G. M. (1998) *Nat. Struct. Biol.* **5,** 903–909
9. Furukawa, K. (1999) *J. Cell Sci.* **112,** 2485–2492
10. Wilson, K. L. (2000) *Trends Cell Biol.* **10,** 125–129
11. Craigie, R., Hickman, A. B., and Engelman, A. (1995) *HIV: A Practical Approach* (Karn, J., ed) Vol. 2, pp. 53–71, Oxford University Press, New York
12. Engelman, A., and Craigie, R. (1995) *J. Virol.* **69,** 5908–5911
13. van Dyke, M. W., Sirito, M., and Sawadogo, M. (1992) *Gene* **111,** 99–104
14. Wetlaufer, D. B. (1962) *Adv. Protein Chem.* **17,** 303–390
15. Chen, H., Wei, S.-Q., and Engelman, A. (1999) *J. Biol. Chem.* **274,** 17358–17364
16. Telesnitsky, A., and Goff, S. P. (1997) *Retroviruses* (Coffin, J. M., Hughes, S. H., Varmus, H. E., eds) pp. 121–160, Cold Spring Harbor Laboratory, Cold Spring Harbor, NY
17. Yang, J. T., Wu, C.-S. C., and Martinez, H. M. (1986) *Methods Enzymol.* **130,** 208–269
18. Hickman, A. B., Palmer, I., Engelman, A., Craigie, R., and Wingfield, P. (1994) *J. Biol. Chem.* **269,** 29279–29287
19. Smith, J. S., and Roth, M. J. (1993) *J. Virol.* **67,** 4037–4049

Both the Structure and DNA Binding Function of the Barrier-to-Autointegration Factor Contribute to Reconstitution of HIV Type 1 Integration *in Vitro*

Dylan Harris and Alan Engelman

J. Biol. Chem. 2000, 275:39671-39677.
doi: 10.1074/jbc.M002626200 originally published online September 25, 2000
